Application of $\mathcal{H}_\infty$ Fault Detection and Isolation to a Boeing 747-100/200 Aircraft

Andrés Marcos *
Subhabrata Ganguli †
Gary Balas ‡
University of Minnesota, Minneapolis.

Fault Detection and Isolation (FDI) methods have been developed over the past thirty years but only in the last several years they have been applied to complex real applications. This paper presents a synthesis of $\mathcal{H}_\infty$ FDI filters for the longitudinal motion of the Boeing 747-100/200 aircraft. The filters are synthesized to detect and isolate faults in the elevator actuator and pitch rate sensor while attenuating disturbances and noise on the fault signals. They are synthesized for open-loop LTI models of the aircraft. Closed-loop simulations with a high-fidelity nonlinear model in the presence of gust and noise are performed to validate the disturbance rejection and robust properties of the $\mathcal{H}_\infty$ LTI FDI filters.

Introduction

In the last thirty years the field of fault detection and isolation (FDI) and the associated fault tolerant control (FTC) have attracted much attention from control engineers, especially in the flight control community. Methods to apply FDI and FTC schemes to control systems abound in the academic literature and some have already been applied to real applications.[1–5] Among these, observer-based approaches have arisen as one of the most widespread, and particularly $\mathcal{H}_\infty$-optimization based methods are increasingly of interest due to the explicit address of robustness issues.

The basic ideas behind observer-based FDI schemes are the generation of residuals, and the use of an optimal or adaptive threshold function to differentiate faults from disturbances.[5–7] Generally, the residuals, also known as diagnostic signals, are generated from estimates of the system's measurements obtained by a Luenenberger observer or a Kalman filter. The threshold function is then used to 'detect' the fault by discretising the residuals from false faults, disturbances and probable faults. For fault isolation the generated residual has to include enough information to differentiate said fault from any other, usually this is accomplished through structured residuals or directional vectors. Robustness of the FDI algorithm is determined by its capability to de-sensitize the filters from disturbances, errors, and model discrepancies.[7–10]

In $\mathcal{H}_\infty$-optimization methods the filtering problem is formulated so that different performance indexes are either minimized or maximized. The FDI filter has two main design goals: to minimize the influence of non-fault signals (noise, disturbances, uncertainties, commands) on the residuals and to maximize isolation of the faults.[5,8,11] These goals are often contradictory since usually a trade-off is required between the residual sensitiveness to faults and its robustness to non-faults. Threshold functions can be used to improve upon the performance of the filter since they can further de-sensitize the residual to non-faults.[5] The application of $\mathcal{H}_\infty$ techniques to FDI parallels the emergence of $\mathcal{H}_\infty$ theory in control design. First, a realization of its power to solve robust problems was appreciated,[12] then it was extended from a factorization perspective,[13] momentum was created by a number of researchers that proposed solutions and applications,[7–10,14] and then more sophisticated extensions of the $\mathcal{H}_\infty$ infinity theory were started to be applied. It is only natural then to progress into $\mathcal{H}_\infty$ gain scheduled and Linear Parameter Varying (LPV) filters, the latter have been treated recently.[15–17]

In this paper, a $\mathcal{H}_\infty$ FDI filter at one point of the flight envelope will be developed based on the open-loop aircraft model (i.e. independent from the controller design process) with the main design goal of being capable of detecting, isolating, and identifying important faults for the longitudinal motion of the Boeing 747 aircraft. The FDI scheme is used to identify faults in the elevator actuator and the pitch rate sensor in the presence of uncertainties such as model errors, gust disturbances and sensor noise. The approach taken is an observer-based fault detection algorithm applying $\mathcal{H}_\infty$ filtering techniques. The problem will be formulated such that the residuals will be sensitive to only one of the faults and both as robust as possible to everything else (model errors, disturbances, noise, ...). In order to analyze the robustness and performance characteristics of the design in the face of plant variations

*Graduate Student, University of Minnesota, Department of Aerospace Eng. and Mechanics. E-mail: marcosa@aem.umn.edu
†Graduate Student, University of Minnesota, Department of Aerospace Eng. and Mechanics.
‡Professor, University of Minnesota, Department of Aerospace Eng. and Mechanics.

the same $\mathcal{H}_\infty$ interconnection and weights will be used to synthesize several more $\mathcal{H}_\infty$ FDI filters throughout the flight envelope. Open-loop and closed-loop analysis will be carried out for the set of FDI filters.

The layout of the paper is as follows. First, a brief theoretical background is given. Then, the nonlinear and linear aircraft models are introduced. The LTI controllers used for closed-loop simulation are presented in the following section. Next, The FDI filter design, interconnection and selection of the adequate weights is covered . Finally, conclusions are drawn and future research directions are given.

$\mathcal{H}_\infty$ Robust Fault Diagnosis Problem

This section presents a brief introduction to the main definitions and goals of $\mathcal{H}_\infty$ fault detection and isolation filters. Figure 1 illustrates the $\mathcal{H}_\infty$ robust fault diagnosis problem. P is a nominal LTI plant, and F is the desired stable $\mathcal{H}_\infty$ filter. The vectors f, d, u correspond to the fault, disturbance and control inputs respectively. The estimation error is given by e, and is the difference between the fault and the residual vector, res. The output from the plant is given by the y vector, and w, z denote the fictitious input and output of the uncertain model, Δ.

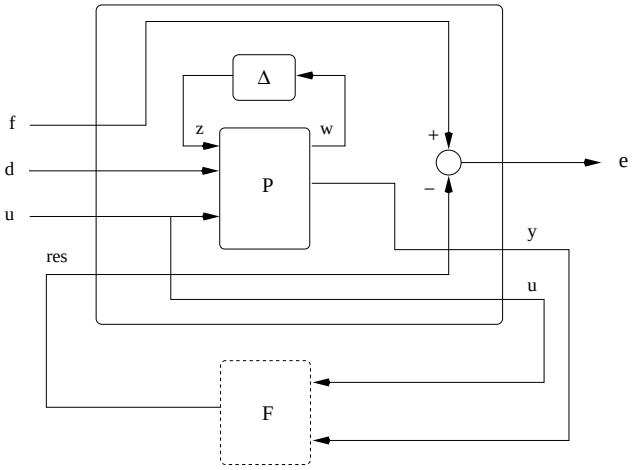

Fig. 1 $\mathcal{H}_\infty$ filter problem with uncertain model.

Let x_p be the plant state vector, and x_f the states for the filter. Then the plant state space representation is given by:

$$\dot{x_p} = A_p\, x_p + B_p\, u + R1_p\ f + E1_p\, d + Q1\, z \qquad (1)$$

$$y = C_p\, x_p + D_p\, u + R2_p\ f + E2_p\, d + Q2\, z \qquad (2)$$

and that of the filter and the estimation error by

$$\dot{x_f} = A_f\, x_f + B1_f\, u + B2_f\, y \qquad (3)$$

$$res = C_f\, x_f + D1_f\, u + D2_f\, y \qquad (4)$$

$$e = M\ f - I\ res \qquad (5)$$

where all the matrices are of appropriate order. All the system matrices are known except for those pertaining to the filter $(A_f, B1_f, B2_f, C_f, D1_f, D2_f)$. The perturbation output, z, in Figure 1, can be considered as a special type of disturbance.[18] The $\mathcal{H}_\infty$ robust fault diagnosis problem is then given by equations $1 \rightarrow 5$. Combine the disturbance, d, and the perturbation output, z, into a generalized disturbance vector, $\bar{d} = [z\ d]$. Then a modified problem can be obtained which is in the standard $\mathcal{H}_\infty$ configuration paradigm,[19] Figure 2.

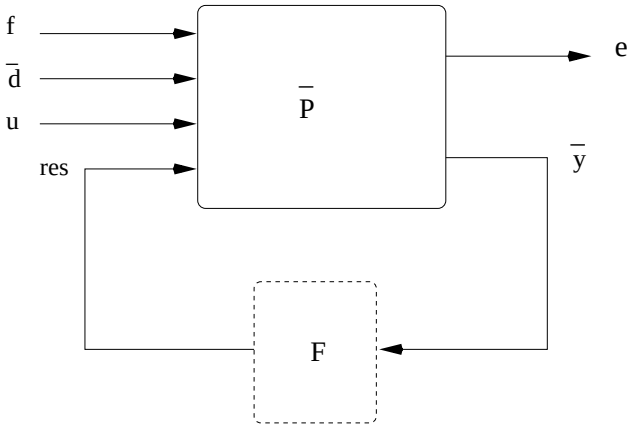

Fig. 2 Modified $\mathcal{H}_\infty$ filter problem.

The objective of the $\mathcal{H}_\infty$ filter synthesis is to find a stable filter that minimizes the transfer function from the disturbances to the errors (i.e min $||TF_{e\,\hat{d}}||_\infty$) while maximizing the faults effect on the errors (i.e. max $||TF_{e\,f}||_\infty$) where $\hat{d} = [\bar{d}\ u]$, see References.[7,10]

Aircraft Models

In this section the aircraft nonlinear and linear time invariant (LTI) models for the longitudinal axis and the turbulence model are presented. A more detailed presentation of the nonlinear model can be found in references.[20,21] The LTI models are used in the design stage while the high-fidelity nonlinear model is used in the closed-loop simulations.

The aircraft model used in this paper is the Boeing 747 series 100/200. The Boeing 747 is an inter-continental wide-body transport with four fan jet engines designed to operate from international airports. Some of its performance characteristics are a range of 6,000 nautical miles, a cruising speed greater than 965 kilometers per hour and a design ceiling of 13,716 meters.

The focus of the paper is on the longitudinal motion of the aircraft. A movable horizontal stabilizer with four elevator segments (i.e. two inboards and two outboards) and the four engines thrust are used to control the longitudinal axis motion. The horizontal stabilizer, δ_s, is only used for trimming purposes. Assuming normal operation of the aircraft, the inboard and outboard elevators move together, hence for our purposes the model will be assumed

to have one elevator surface, δ_e. The aerodynamic data for the Boeing 747-100/200 aircraft was obtained from references.[22,23] This data was simplified through an analytical study of each stability derivative and open-loop simulations of the resulting low-fidelity nonlinear model. The details of these studies are found in reference.[20] The nonlinear low fidelity model is then used to obtain linear time invariant (LTI) models.

The nonlinear body-axes longitudinal motion of the Boeing 747, not including flexible effects, can be described by the following differential equations.

$$\dot{\alpha} = \frac{[-F_x \cdot s_\alpha + F_z \cdot c_\alpha]}{m \cdot V_{TAS}} + q \tag{6}$$

$$\dot{q} = c_7 \cdot M_y \tag{7}$$

$$\dot{\theta} = q \tag{8}$$

$$\dot{V_{TAS}} = \frac{1}{m} \cdot [F_x \cdot c_\alpha + F_z \cdot s_\alpha] \tag{9}$$

$$\dot{h_e} = V_{TAS} \cdot c_\alpha \cdot s_\theta - V_{TAS} \cdot s_\alpha \cdot c_\theta \; = \; V_{TAS} \cdot sin\gamma \tag{10}$$

The body-axes aerodynamic forces and moments are given by

$$F_x = \; -\bar{q}S \cdot [C_D \cdot c_\alpha - C_L \cdot s_\alpha] + \sum_{i=1,4} Tn_i - mg \cdot s_\theta \tag{11}$$

$$F_z = \; -\bar{q}S \cdot [C_D \cdot s_\alpha + C_L \cdot c_\alpha] - 0.0436 \cdot \sum_{i=1,4} Tn_i + mg \cdot c_\theta \tag{12}$$

$$M_y = \bar{q}S\bar{c} \cdot \{C_m - \frac{1}{\bar{c}}[(C_D \cdot s_\alpha + C_L \cdot c_\alpha) \cdot \bar{x}_{cg} - (C_D \cdot c_\alpha - C_L \cdot s_\alpha) \cdot \bar{z}_{cg}] + \frac{\bar{c}\dot{\alpha}}{V_{TAS}}[C_{m_{\dot{\alpha}}} - \frac{\bar{x}_{cg}}{\bar{c}} \cdot C_{L_{\dot{\alpha}}} \cdot c_\alpha]\} + \sum_{i=1,4} Tn_i \cdot zeng_i \tag{13}$$

The LTI models are obtained through Jacobian linearisations of the nonlinear model at different points in the flight envelope of interest ($he \in$ [4000,10000] m, $Vtas \in$ [150,250] m/s). These LTI models will be used in the FDI filter design stage. Table 1 shows the trim points in the flight envelope used for design and LTI simulation.

point	altitude, m	airspeed, m/s	Mach number
1	4000	184	0.567
2	4000	232	0.71
3	9250	125	0.71
4	9250	247	0.81
5	7000	241	0.77

Table 1 Trim points.

The longitudinal axis LTI aircraft model used for the filter design has five states : pitch rate q (rad/s), true airspeed $Vtas$ (m/s), angle-of-attack α (rad), pitch angle θ (rad), and altitude he (m). There are three control inputs: elevator deflection δ_e (rad), stabilizer deflection δ_s (rad) (always set to the corresponding trim value) and thrust Tn (N).The measurements available are flight path angle (FPA) γ (rad), acceleration $\dot{V}$ (m/s^2/g), pitch angle (rad), pitch rate (rad/s), velocity (m/s), and altitude he (m).

The deflection and rate limits for the elevator are -23 to 17 deg and ± 37 deg/s respectively as specified in reference.[23] For the stabilizer the position and rate limits are -12 to 3 deg and 0.5 deg/s respectively.[23] Taking the rate limits into account, the elevator and stabilizer are modeled as simple first-order transfer functions: $37/(s+37)$ and $0.5/(s+0.5)$ respectively. The engine dynamics are modeled as $0.5/(s+0.5)$ based on the engine transient characteristics provided in reference.[23] The sensors are considered to be ideal, hence the plant inputs are fed back directly to the filter or the controller corrupted only by noise during simulation.

The closed-loop simulations will be corrupted by noise in the sensors and by a turbulence model entering the nonlinear aircraft model through the stability derivatives. The implementation of a realistic turbulence model is carried out by using two-dimensional autocovariance functions. These functions represent the statistical properties of the atmospheric turbulence for a two dimensional stationary, homogeneous and isotropic field of flow. It is an enhancement over the typical one-dimensional flow in that the gust velocity changes in the horizontal plane both along the X_{earth} and Y_{earth} axes (the Z_{earth} is considered negligible due to the relative size of the aircraft along this axis). Basically, turbulence is simulated by feeding white noise through stable, minimum-phase Dryden Spectra filters to the system. For the longitudinal (symmetric) and lateral (asymmetric) motions of an aircraft in turbulence the model developed at Delft University of Technology was followed (see reference[24] for an excellent report on the characteristics of turbulence and its implications to aircraft flight).

In Table 2, a summary of the turbulence parameters values (variance of x, σ_x^2, and turbulence scale, L_g) are given for light, moderate and severe turbulence for medium and high altitude flight (see references[25,26]).

turbulence	altitude	σ (m/s)	L_g (m)
Light	$600 \leq$ he ≤ 2800	1.55	$L_g = 530$
	$2800 \leq$ he ≤ 5100	$2.32 - 0.000274 \cdot$ he	idem
	he ≥ 5100	0.92	idem
Moderate	$600 \leq$ he ≤ 3400	3.05	idem
	he > 3400	$3.84 - 0.000234 \cdot$ he	idem
Severe	$600 <$ he < 1400	$3.04 + 0.00244 \cdot$ he	idem
	$1400 \leq$ he ≤ 5800	6.45	idem
	he > 5800	$8.40 + 0.000336 \cdot$ he	idem

Table 2 Turbulence Parameters for medium to high altitudes.

Controller

For closed-loop simulations LTI $\mathcal{H}_\infty$ controllers obtained at the same trim points as the $\mathcal{H}_\infty$ FDI filters are used (see Table 1). This section outlines a brief sketch of the LTI control synthesis, a more thorough presentation is given in reference.[27]

In the aforementioned reference, a reconfigurable LPV controller for the longitudinal motion of the Boeing 747-100/200 is presented. The LPV controller has the particularity of scheduling on true airspeed, altitude and the fault signal produced by the FDI filter presented in this paper. For closed-loop simulation of the FDI filter, LTI controllers are obtained from the LPV controller at several points in the flight envelope for the non-fault case (i.e. there is no reconfiguration due to the occurrence of faults).

The controller objectives are to achieve de-coupled tracking of flight-path angle (FPA) and velocity with settling times of 15 sec and 45 sec respectively with the elevator surface fully functional, and the rejection of gust disturbances for the Up-and-Away flight envelope.

The controller has five measurements available: flight path angle (FPA) γ (rad), acceleration $\dot{V}$ (m/s^2/g), pitch angle (rad), pitch rate (rad/s), and velocity (m/s). There are two control outputs: elevator deflection δ_e (rad), and thrust Tn (N). The stabilizer δ_s is always set to trim in the non-fault case.

FDI Filter Design

This section presents the design of the $\mathcal{H}_\infty$ FDI filters. First, the formulation of the filtering problem is presented. Then, a detailed description of the weights used to achieve the performance and robustness objectives is given. Finally, the open-loop and closed-loop simulations are presented.

FDI Filter Formulation

It is well known, see references,[7,10,17] that the FDI filtering problem can be posed as a standard $\mathcal{H}_\infty$ filtering problem.Hence, by translating performance objectives into filtering objectives and robustness issues into the classical disturbance rejection (whether these are noise or modeling errors) it is possible to use the available information and experience from control design in filtering design.

The main philosophy behind the filter design formulation in this paper is that of model matching with tracking (detection for the FDI filter) requirements. These objectives are in accordance with standard requirements for FDI filters.The filters must be able to detect and isolate different failure signals (i.e. elevator actuator and pitch rate sensor) which is similar to a de-coupled tracking problem from the control's point of view. An important characteristic of a FDI filter is its capability to distinguish between the failure signatures and any other signal (noise, gust, control inputs, ...), thus the FDI filters should include disturbance attenuation properties. It is possible to view the disturbance rejection as a robustness problem in the sense that the filter is robust to the influence of non-fault signals. It can be argued that modeling errors fall into this category, and hence that the filter is effectively robust. The faults are assumed to enter the system in an additive manner: e.g. $\delta_e = u_{actuator} + f_a$.

The filter design is carried out for one point in the flight envelope (specifically for point number 1, low speed and low altitude, in Table 1). Then, the same interconnection structure and weights are used to synthesize the other points in the afore mentioned Table. Open-loop and closed-loop simulations are obtained for the set of points in order to analyze the performance and robustness characteristics in the face of plant variations.

The FDI $\mathcal{H}_\infty$ filtering interconnection is shown in Figure 3. The vector y is formed by the feedback signals from the plant (i.e. γ, $\dot{V}$, θ, q, $Vtas$ and he); the disturbance vector is given by d and consists of noise for each feedback channel. The control inputs are the elevator deflection and thrust, $u = [\delta_e \;\; Tn]$. Two faults are modeled, one for the elevator actuator, fa and the other in the pitch rate sensor, fs, hence $f = [fa \;\; fs]$; and equivalently the residual vector is then given by $res = [res_{act} \;\; res_{sen}]$. The uncertainty input and output channels are represented respectively by w and z. Selection of the weights is one of the most critical steps, through them is possible to shape the frequency spectrum of the signals and thus make the system (in the present case the filter) behave as desired. As seen in the interconnection shown in Figure 3, there are four different sets of weights: uncertainty W_{unc}, disturbance W_{dist}, fault W_{fault} and estimated error W_{error}.

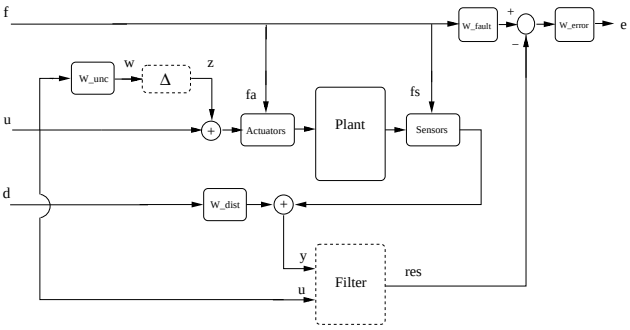

Fig. 3 $\mathcal{H}_\infty$ Filter Interconnection.

A multiplicative uncertainty setup is used to try to address uncertainty in the augmented plant (plant, actuator and sensors). The weights are chosen as constants representing a 50 percent uncertainty at actuator input: $W_{ele_{unc}} = W_{thrust_{unc}} = 0.5$. A high-pass type of weight was also tested but it was found that the gain of the weight at high frequencies was forcing the γ-iteration for the

$\mathcal{H}_\infty$ synthesis to stop at that value, i.e. $\gamma = W_{unc}(\infty)$, and consequently the FDI filter could not be improved further.

The disturbance weights are used to attenuate the disturbance effects on the fault estimation. The final weights were achieved in a heuristic manner by starting with typical shapes of the Sensitivity function, S, for flight control systems and then analyzing the effect on the LTI and nonlinear closed loop. Since the faults are assumed to enter in an additive manner, the q weight is critical in shaping the response of the FDI filter. Its gain and corner frequencies were found to be directly connected to the response of the sensor residual. Figure 4 show the frequency responses of the different disturbance weights, and the corresponding transfer functions are given below.

$$W_{\gamma_{dist}} = \frac{0.1}{57.3}\frac{\frac{s}{0.01}+1}{\frac{s}{50}+1} \qquad W_{\dot{V}_{dist}} = 0.1\frac{\frac{s}{0.01}+1}{\frac{s}{50}+1} \tag{14}$$

$$W_{\theta_{dist}} = \frac{0.1}{57.3}\frac{\frac{s}{0.09}+1}{\frac{s}{40}+1} \qquad W_{q_{dist}} = 0.5\,\frac{s+1}{\frac{s}{100}+1} \tag{15}$$

$$W_{V_{dist}} = 0.05\frac{\frac{s}{0.1}+1}{\frac{s}{50}+1} \qquad W_{he_{dist}} = 100\frac{\frac{s}{0.01}+1}{\frac{s}{50}+1} \tag{16}$$

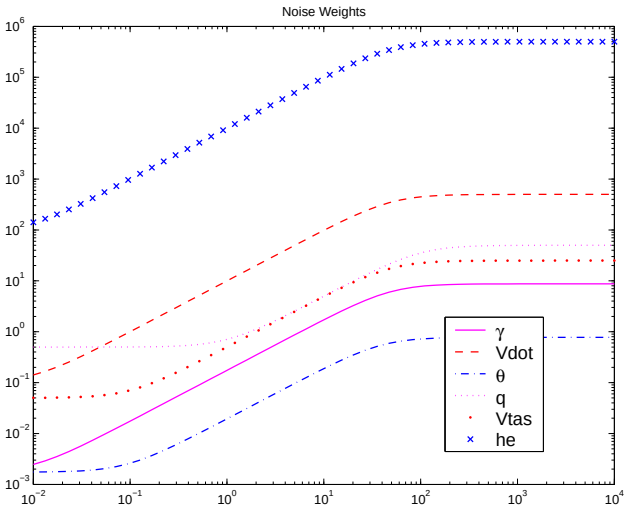

Fig. 4 Disturbance Weights.

The faults are filtered before entering the estimation error equation, this is becoming a common fixture in $\mathcal{H}_\infty$ FDI techniques, see references.[7,10,17,28] It is akin to the well-known model matching problem in control.[19,29] As such, these weights are the knobs used by the filter designer to shape the response of the residuals. The choice of weights is driven by the need to provide good detection characteristics for the residuals and a sufficiently fast response to fault signals. They correspond to a rise time of 3 to 6 seconds for the actuator and sensor residual respectively. The gains are fine tuned after selecting the noise weights so that there will be no steady state error in the fault detection. As mentioned before the gain for the sensor residual is directly tied to the gain of the pitch rate noise weight. One can achieve faster responses (down to milliseconds) at the expense of the disturbance rejection properties of the filter and to coupling between the residuals. Hence, there is a direct trade-off between the fault detection time domain characteristics as rise time and steady state error (filter performance) and fault disturbance rejection (filter robustness). The weights are given below and the corresponding frequency responses are shown in Figure 5.

$$W_{act_{fault}} = 2\,\frac{\frac{s}{300}+1}{\frac{s}{2}+1} \qquad W_{sen_{fault}} = 1.25\,\frac{\frac{s}{300}+1}{s+1} \tag{17}$$

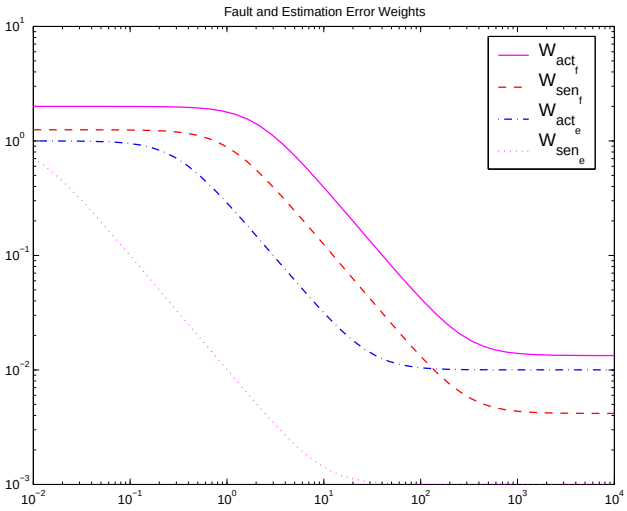

Fig. 5 Filtered Fault and Estimation Error Weights.

The last set of weights correspond to the estimation errors. Recall, that the estimation error, equation 5, is the difference between the filtered fault and the residual. The de-coupling of the residuals is achieved by penalizing both errors. The estimation error weights parallel the performance weights in the standard control set-up. The idea is to minimize the error at low frequencies and relax the constraints at higher frequencies. Hence low pass weights are selected for the actuator and sensor errors. Interestingly, it was noticed that the zeros of the weights showed up as poles of the filter and hence they were selected to be small to avoid high frequency poles. The weights are shown in Figure 5.

$$W_{act_{error}} = \frac{\frac{s}{30}+1}{\frac{s}{0.3}+1} \qquad W_{sen_{error}} = \frac{\frac{s}{10}+1}{\frac{s}{0.01}+1} \tag{18}$$

Sensor failures are intrinsically easier to detect and isolate[7] since they enter directly into the filter. Thus it is possible to get away often with constant gain or less stringent frequency weights enabling the filter designer to focus in the actuator faults and the disturbance rejection. This was especially true in the present case since the

sensors were assumed to be ideal which simplified our task. The weight selection was driven by the actuator fault residual and its disturbance characteristics.

In selecting the input channels to the filter we started assuming the same channels as for the controller (γ, $\frac{\dot{V}}{g}$, θ, q and $Vtas$) plus the controller outputs (δ_e and Tn) in the assumption that in a real implementation it will be easier and economically more meaningful to use available sensors. Even though it was possible to obtain an acceptable level of performance for the FDI filters with these inputs the robustness characteristics were much poorer. Introducing altitude as an additional input to the filter improved its robustness. This is reasonable since the more information the filter has of the plant behavior the better its performance, especially since altitude and velocity are the primary parameters that affect plant dynamics.

Simulations and Analysis

In the following simulations we will refer to the open/closed loop as LTI whenever a LTI plant model is used and as nonlinear open/closed loop when the nonlinear aircraft model is being used. Also, note that for the closed-loop case, whether LTI or nonlinear, the controller used is a LTI $\mathcal{H}_\infty$ controller obtained at the same design point as for the $\mathcal{H}_\infty$ FDI filter used in that particular simulation.

First, the LTI open-loop behavior of the FDI filters is analyzed. Figure 6 shows the residual responses of the 5 FDI filters (obtained at the 5 trim points given in Table 1) to a 2 deg step input of the elevator at $t = 25$ sec and a 300 Newtons step in the thrust channel at $t = 30$ sec. The faults considered in this open-loop simulation (the same will be used in the sequel) are not realistic in the sense that is unlikely that a fault in the actuator or the sensor will show this type of behavior, they are shown in Figure 6 by the solid red line. This convoluted set of faults inputs is introduced in order to differentiate the effect of each fault in the plant outputs while testing the coupling between the faults.

The previous LTI open-loop simulations are performed without disturbances (neither gust nor noise inputs) or modeling errors (they are LTI models). Since there are no modeling errors or uncertainties the responses of the 5 filters are indistinguishable from one another (introducing gust and noise did not changed the similarity in the responses). This is expected since in the LTI open-loop simulation all the issues related to changes in the trim points and to uncertainty are discarded by means of the LTI nature of the simulation. The filters have the desired dynamic behavior: rise times of 3 to 6 seconds, de-coupling of the residuals, detection of the faults, and rejection of disturbances (in this case the commands).

Figure 7 shows the plant responses, plant inputs and

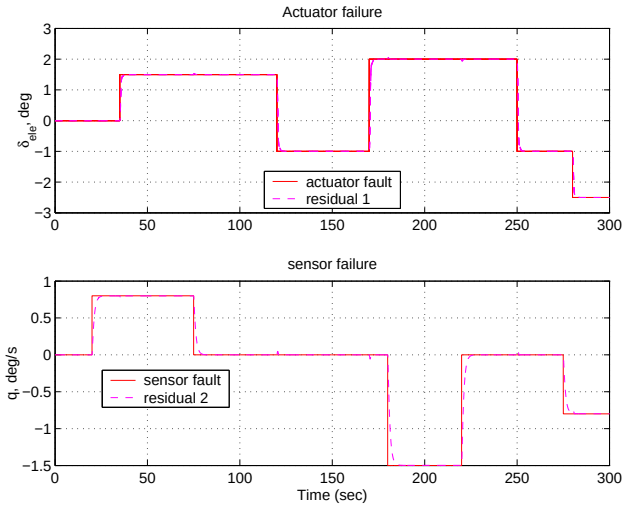

Fig. 6 Plant inputs - LTI Open Loop.

filter residuals for the LTI closed loop at the 5 design points. The commands to the controller are a -2 deg γ square input from $t = 15$ to $t = 60$ sec, and a square $Vtas$ of 15 m/s starting at $t = 16$ and ending at $t = 130$ sec. The residuals responses are identical to those for the LTI open-loop (Figure 6) due to the non-uncertainty in the simulations (see reference[30] for a theoretical explanation). The sensor fault has a negligible coupling effect on the actuator residual, but it has a much greater effect on some of the plant outputs (especially in the flight path angle). This is natural since sensor faults affects primarily the controller behavior which uses the pitch rate as one of the feedback channels (observe how the elevator output from the controller shows substantial peaks at the times the sensor fault is introduced). From Figure 7 this feedback relation is easily observed, the moment the sensor fault enters in the system the controller reacts in an impulsive manner (i.e. it reacts by commanding a high demand of the elevator in a very short time) which in turn produces high peaks in the θ, q and γ outputs. Since the θ and q channels are intrinsically related this means that the choice of the corresponding disturbance weights, $W_{\theta_{dist}}$ and $W_{q_{dist}}$, and the actuator estimated error weight, $W_{act_{error}}$, are going to affect each other. The actuator fault has a similar effect, although less dramatic, in the plant outputs and also a small noticeable effect on the sensor residual.

The next step is to simulate the $\mathcal{H}_\infty$ FDI filters in the nonlinear closed loop. As mentioned before, in this case the plant is the nonlinear high-fidelity model (this will enable to test for model discrepancies with respect to the linear plants used in the design procedure). Figure 8 shows the residuals of the nonlinear close-loop simulation for all the trim points. The manoeuvre performed is a steadily accelerated climb performed by commanding a 3 deg square flight path angle from $t = 15$ to $t = 95$ and a velocity step command of 18 m/s starting at $t = 20$ sec. It is observed that as expected the sensor residual is much more efficient and robust with respect to plant variations.

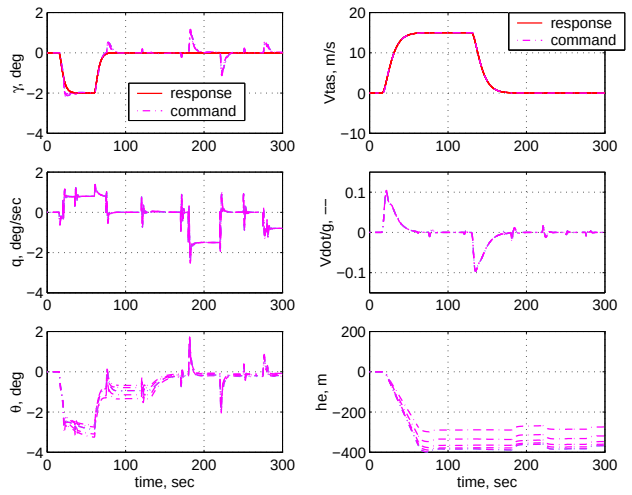

a) Plant responses.

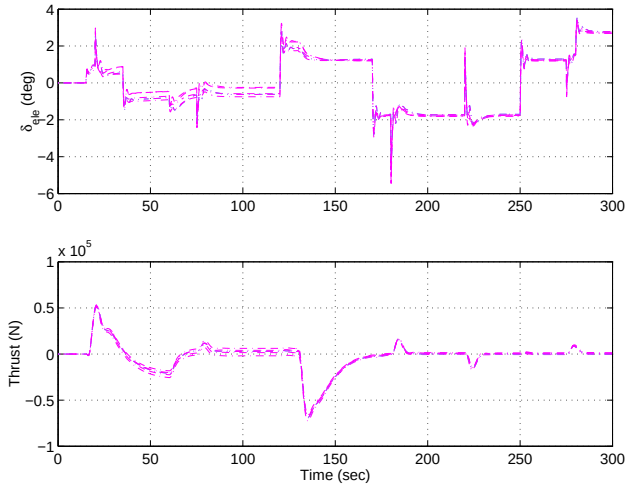

b) Plant inputs.

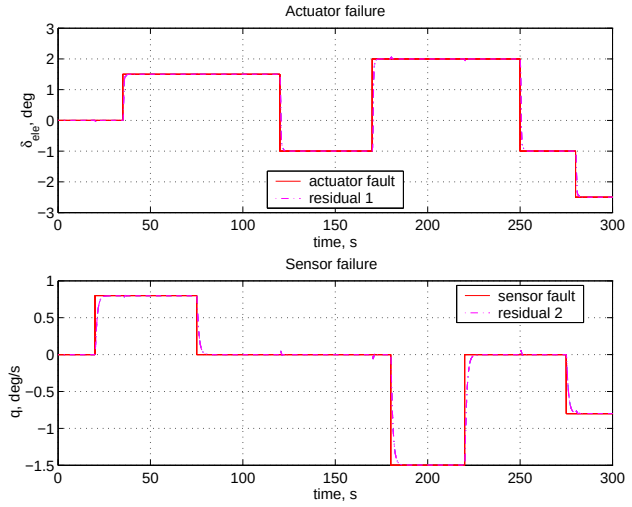

c) Filter residuals.

Fig. 7 Plant responses, inputs and filter residuals - LTI closed loop all points.

The actuator residual shows good detection capabilities but is clearly more affected by plant variations, specially in the high speed and high altitude region. This is also expected since the $\mathcal{H}_\infty$ weights were obtained for a low speed, low altitude condition (specifically point 1) and then finally fine tuned to obtain acceptable behavior at the other points. This is an inherent limitation of LTI techniques, but it could be improved by using more sophisticated techniques as gain scheduling or LPV synthesis; it could also be improved by using adaptive thresholds to remove the effect produced by the commands (basically the change in trim). Also, the effect of the 2nd square sensor fault (at $t = 250$ and $t = 280$) is more pronounced in the actuator residual. This is due to the magnitude of the sensor fault, a 1.5 degree fault in the pitch rate sensor is quite strong almost a failure. As mentioned before, this sensor fault produces a high demand of control authority in the elevator channel that gets transmitted down to the plant outputs and to the filter where the residual of the elevator shows relatively big transients at those times.

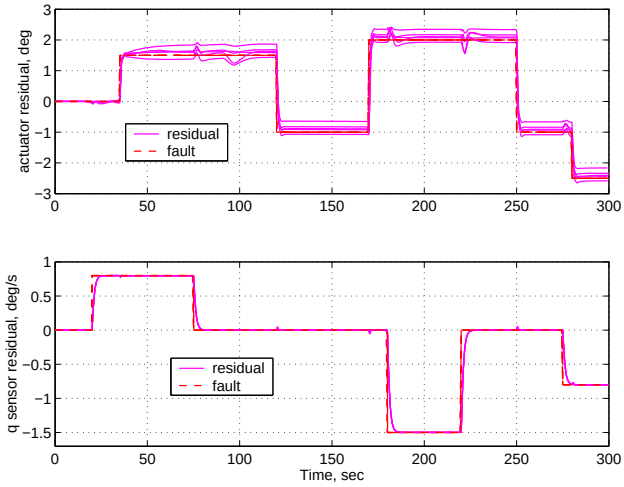

Fig. 8 Residuals - Nonlinear Closed Loop for all points.

The robustness of the filters to external disturbances is tested by using the turbulence model given before and white noise inputs added to the plant outputs (the sensors are considered to be ideal). A moderate level of turbulence is selected ($L_g = 530$ m and $\sigma = 3.84 - he\ 0.000234$ m/s). The noise is given by a uniformly distributed random number generator (a standard SIMULINK© block) with initial seed of 0 and a minimum/maximum interval of $\pm$ 0.1 deg for the γ and θ channels, $\pm$ 0.1 deg/sec for the pitch rate, $\pm\ 0.1/g$ for the acceleration, $\pm$ 0.2 m/s for the true airspeed and $\pm$ 10 m for the altitude.

In Figures 9 $\rightarrow$ 11 the nonlinear closed-loop responses with gust and noise for the $\mathcal{H}_\infty$ FDI filter design at point number 5 of the flight envelope are given. The simulation is affected by moderate turbulence and noise as defined above. Therefore, the disturbance rejection properties and the modeling robustness can be addressed through the sim-

ulation analysis. The manoeuvre performed is the same as before, a steadily accelerated climb that will take the aircraft in this instance one flight level up (from 7000 m up to 8000 m) and accelerate it from 240 m/s to 258 m/s (from Mach=0.77 to Mach=0.84). It can be seen that the disturbance rejection properties are acceptable although the actuator residual has degraded capabilities with respect to the sensor residual.

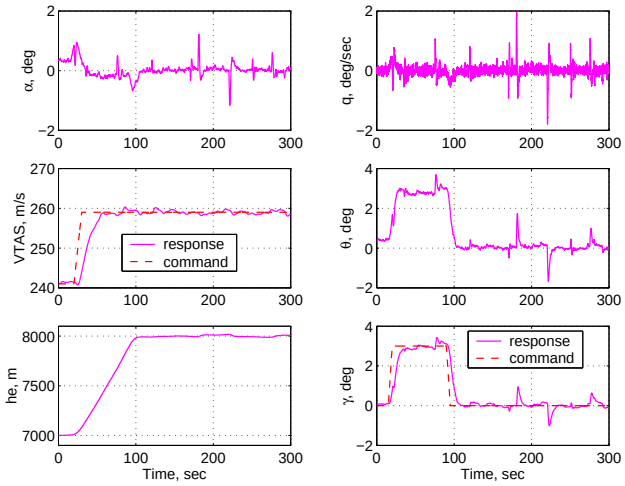

Fig. 9 Plant responses - Nonlinear Closed Loop with Moderate gust and noise (point 5).

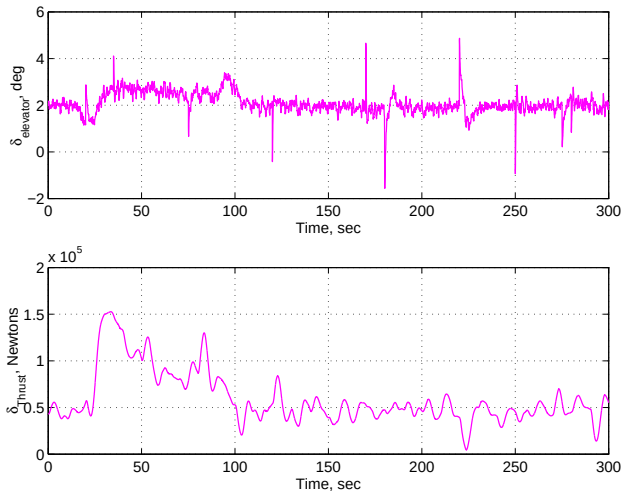

Fig. 10 Plant inputs - Nonlinear Closed Loop with Moderate gust and noise (point 5).

The $\mathcal{H}_\infty$ γ - iteration level obtained for the LTI FDI filter at that design point is 1.414 and the filter has 17 states. The filter residuals are able to detect and isolate the fault signatures with a high degree of accuracy distinguishing at the same time from control inputs and disturbances effects. The jittery behavior of the residuals (mainly due to the noise and gust effects) is relatively small and does not prevent the filter from detecting the faults. An adaptive threshold[5–7] could be added to increase the likelihood of identifying soft faults and missed faults. The

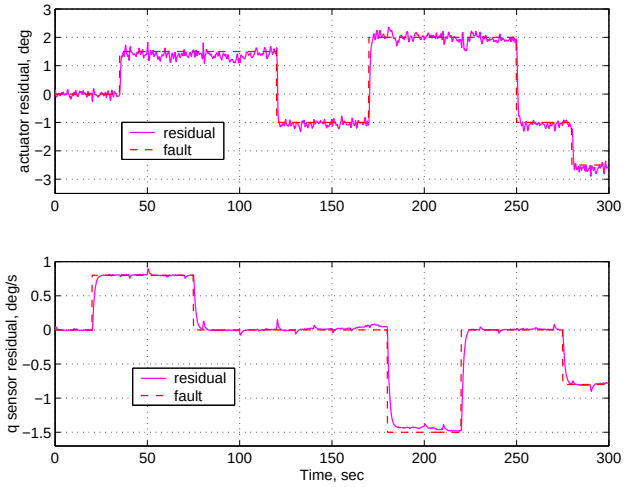

Fig. 11 Residuals - Nonlinear Closed Loop with Moderate gust and noise (point 5).

controller succeeds in providing smooth tracking of the *Vtas* command as expected, while the flight path angle tracking is much more sensitive to the effects of faults but yet robust enough to handle non-critical faults.

Conclusions

In this paper, it has been shown an application of $\mathcal{H}_\infty$ Fault Detection and Isolation filter techniques to a high-fidelity model of the Boeing 747-100/200 aircraft. Ad-hoc analyses of the robustness properties and disturbance rejection capabilities of the LTI filters have been obtained through open-loop and closed-loop simulations. The $\mathcal{H}_\infty$ FDI filters thus obtained are capable of detecting and isolating faults in the elevator actuator and the pitch rate sensor.

The next natural step is to use available LPV control synthesis techniques to synthesize an LPV FDI filter. Parallelism drawn throughout the paper with standard $\mathcal{H}_\infty$ control techniques and the $\mathcal{H}_\infty$ filtering design enable us to view this as a promising path which we hope to incorporate in a future paper.

Acknowledgments

This research was supported under NASA Langley Cooperative Agreement No. NCC-1-337, technical contract monitor Dr. Christine Belcastro. The authors wish to thank the faculty of the Aerospace department at Delft University in The Netherlands for the availability of the lecture notes on turbulence and the original software for the Boeing 747-100/200 aircraft.

References

[1]Blanke, M., Izadi-Zamanabadi, R., Bogh, S.A., and Lunau, C., "Fault Tolerant Control Systems - A Holistic View," *Control Engineering Practice*, Vol. 5, No. 5, May 1997, pp. 693–702.

[2]Blanke, M., Staroswiecki, M., and Wu, N.E., "Concepts and Methods in Fault-tolerant Control," *Proceedings of the American Control Conference*, Arlington, VA, June 2001.

[3]Isermann, R., "Supervision, Fault-Detection and Fault-Diagnosis Methods - An Introduction," *Control Engineering Practice*, Vol. 5, No. 5, 1997, pp. 639–652.

[4]Patton, R.J., "Fault-Tolerant Control Systems: The 1997 Situation," *IFAC SAFEPROCESS'1997*, Hull, UK, August 1997.

[5]Frank, P.M. and Ding, X., "Survey of Robust Residual Generation and Evaluation Methods in Observer-Based Fault Detection Systems," *Journal of Process Control*, Vol. 7, No. 6, 1997, pp. 403–424.

[6]Frank, P.M. and Ding, X., "Frequency Domain Approach to Optimally Robust Residual Generation and Evaluation for Model-based Fault Diagnosis," *Automatica*, Vol. 30, No. 5, 1994, pp. 789–804.

[7]Patton, R.J. and Chen, J., "Observer-Based Fault Detection and Isolation: Robustness and Applications," *Control Engineering Practice*, Vol. 5, No. 5, 1997, pp. 671–682.

[8]Edelmayer, A., Bokor, J., and Keviczky, L., "An H-infinity Filtering Approach to Robust Detection of Failures in Dynamical Systems," *Proceedings of the 33rd IEEE Conference on Decision and Control*, Vol. 3, Lake Buena Vista, FL, USA, 1994, pp. 3037 –3039.

[9]Mangoubi, R.S., Appleby, B.D., Verghese, G.C., and Vander Velde, W.E., "A Robust Failure Detection and Isolation Algorithm," *Proceedings of the 34th IEEE Conference on Decision and Control, 1995, New Orleans, USA*, Vol. 3, 1995, pp. 2377 –2382.

[10]Stoustrup, J., Grimble, M.J., and Niemann, H., "Design of Integrated Systems for the Control and Detection of Actuator/Sensor Faults," *Sensor Review*, Vol. 17 (2), July 1997, pp. 138–149.

[11]Niemann H.H., Saberi A., Stoorvogel A.A., and Sannuti P., "Optimal Fault Estimation," *IFAC SAFEPROCESS'2000*, Budapest, Hungary, June 2000, pp. 262–267.

[12]Viswanadham, N. and Minto, K.D., "Robust observer Design with Application to Fault Detection," *Proceedings of the American Control Conference*, Atlanta, GA, June 1988, pp. 1393–1399.

[13]Ding, X. and Frank, P.M., "Fault Detection via Factorization Approach," *Systems and Control Letters*, Vol. 14, 1990, pp. 431–436.

[14]Qiu, Z. and Gertler, J., "Robust FDI Systems and H-infinity Optimization: Disturbances and Tall Fault Case," *IEEE Proceeding of the Conference on Decision and Control*, Vol. 2, San Antonio, TX, USA, December 1993, p. 1710 1715.

[15]Bokor, J. and Balas, G.J., "Detection Filter Design with the LPV Framework," *Proceedings of the 19th Digital Avionics System Conference (DASC)*, Vol. 2, Philadelphia, PA, Oct 2000, pp. 6.A.3–1 to 6.A.3–5.

[16]Balas, G.J. and Bokor, J., "Detection Filter Design for LPV Systems," *IFAC SAFEPROCESS'2000*, Vol. 2, Budapest, Hungary, June 2000, pp. 653–656.

[17]Abdalla, M.O., Nobrega, E.G., and Grigoriadis, K.M., "Fault Detection and Isolation Filter Design for Linear Parameter Varying Systems," *Proceedings of the American Control Conference*, Arlington, VA, June 2001.

[18]Chen, J. and Patton, R.J., "$\mathcal{H}_\infty$ Formulation and Solution for Robust Fault Diagnosis," *14th Triennial World Congress of IFAC*, Beijing,P.R.Chine, 1999, pp. 127–132.

[19]Zhou, K., Doyle, J.C., and Glover, K., *Robust and Optimal Control*, Prenticel-Hall, Englewood Cliffs, NJ, 1996.

[20]Marcos, A., *A Linear Parameter Varying Model of the Boeing 747-100/200 Longitudinal Motion*, Master's thesis, Department of Aerospace and Engineering Mechanics, University of Minnesota, 2001.

[21]Marcos, A. and Balas,G., "Linear Parameter Varying Modeling of the Boeing 747-100/200 Longitudinal Motion," *AIAA 2001 Guidance, Navigation, and Control Conference, AIAA-01-4347*, Montreal, Canada, August 2001.

[22]Hanke, C., " The Simulation of a Large Jet Transport Aircraft. Volume I: Mathematical Model," Tech. Rep. NASA CR-1756, The Boeing Company, 1971.

[23]Hanke, C. and Nordwall, D., " The Simulation of a Jumbo Jet Transport Aircraft. Volume II: Modeling Data," Tech. Rep. NASA CR-114494/D6-30643-VOL-2, The Boeing Company, 1970.

[24]Mulder, J.A. and van der Vaart, J.C., "Aircraft Responses to Atmospheric Turbulence," Tech. Rep. Lectures Notes D-4, Delft University of Technology, Delft, The Netherlands, 1998.

[25]MIL-F-8785C, "Military specification - Flying qualities of piloted airplanes," Tech. rep., Department of Defense, November 1980.

[26]Flight Mechanics Action Group 08 and Helmersson, A., "Robust Flight Control Design Challenge Problem Formulation and Manual: the Research Civil Aircraft Model (RCAM)," Tech. Rep. TP-088-03, GARTEUR, February 1997.

[27]Ganguli, S., Marcos, A., and Balas,G.J., "Reconfigurable LPV Control Design for Boeing 747-100/200 Longitudinal Axis," *Proceedings of the American Control Conference*, Anchorage, AK, May 2002.

[28]Stoustrup, J. and Niemann, H., "Application of an H-infinity Based FDI and Control Scheme for the Three Tank System," *Proceedings of IFAC Symposium on Fault Detection, Supervision and Safety for Technical Processes*, June 2000, pp. 268–273.

[29]Doyle, J., Francis, B., and Tannenbaum, A., *Feedback Control Theory*, MacMillan Publishing Co., 1990.

[30]Niemann, H. and Stoustrup, J., "Robust Fault Detection in Open vs. Closed Loop," *Proceedings of 36th IEEE Conference on Decision and Control*, San Diego, California, Dec. 1997, pp. 4496–4497.